



# The Alkaline Leaching Behavior of Silica Solid Solutions in the Product Obtained by Roasting the Mixture of High-Alumina Coal Gangue and Hematite

Xiao-bin Li<sup>1</sup> · Peng Wang<sup>1</sup> · Hong-yang Wang<sup>1,2</sup> · Qiu-sheng Zhou<sup>1</sup> · Tian-gui Qi<sup>1</sup> · Gui-hua Liu<sup>1</sup> · Zhi-hong Peng<sup>1</sup> · Yi-lin Wang<sup>1</sup> · Lei-ting Shen<sup>1</sup>

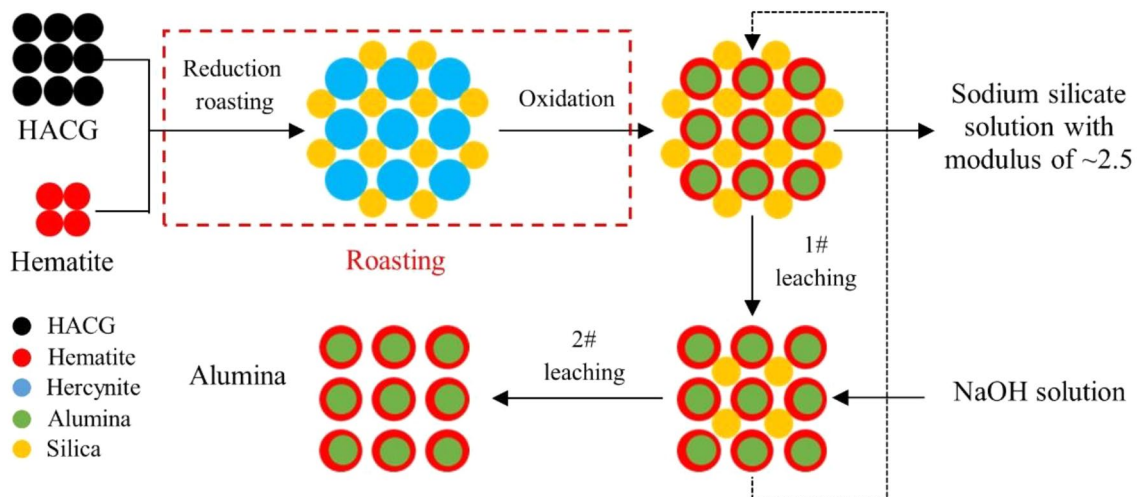
Received: 11 July 2022 / Accepted: 8 October 2022 / Published online: 26 October 2022

© The Minerals, Metals & Materials Society 2022

## Abstract

A novel technology of hematite involved roasting-alkaline leaching-Bayer digestion process was proposed to extract alumina from high-alumina coal gangue (HACG), however the resource utilization of silica was not yet resolved. In this work, the alkaline leaching behavior of silica solid solutions in the product obtained by roasting the mixture of HACG and hematite was systematically studied in sodium hydroxide solution and sodium silicate solution, meanwhile the phase transformation was investigated by X-ray diffraction (XRD), X-ray photoelectron spectroscopy (XPS), scanning electronic microscope (SEM), and energy dispersive spectrometer (EDS). The results show that kaolinite, which is the main mineral in HACG, was converted into silica solid solutions (i.e., quartz solid solution and cristobalite solid solution) and alumina (i.e.,  $\theta$ - $\text{Al}_2\text{O}_3$  and  $\alpha$ - $\text{Al}_2\text{O}_3$ ) through reductively roasting with hematite followed by oxidation during cooling process. Elevated oxidation temperature promotes the conversion of  $\theta$ - $\text{Al}_2\text{O}_3$  into  $\alpha$ - $\text{Al}_2\text{O}_3$ . The silica solid solutions were readily soluble in sodium hydroxide solution and sodium silicate solution while  $\alpha$ - $\text{Al}_2\text{O}_3$  was stable, hence, efficient separation of silica and alumina. Through leaching in sodium silicate solution with a modulus of  $\sim 1.0$  followed by sodium hydroxide solution, a sodium silicate solution with a modulus of  $\sim 2.5$  was obtained together with an alumina concentrate with a mass ratio of alumina to silica of  $> 18.0$ . The alumina concentrate is a decent raw material for alumina extraction by Bayer digestion, and the sodium silicate solution with a modulus of  $\sim 2.5$  can be used in the chemical industry.

## Graphical Abstract



The contributing editor for this article was Atsushi Shibayama.

Extended author information available on the last page of the article

**Keywords** High-alumina coal gangue · Hematite involved roasting · Silica solid solutions · Alkaline leaching · Sodium silicate solution

## Introduction

At present, bauxite is used as the main material for alumina production on a commercial scale. However, about 90% of the bauxite distributes in the Equator and Southern Hemisphere [1]. The bauxite reserve in the main aluminum-producing countries, such as China, the USA, and Russia, only accounts for 5% of bauxite in the world. Therefore, these countries must find alternatives to bauxite for alumina production. Fortunately, the coal reserve is rich in China, the USA, and Russia, and accounts for 13.2%, 23.70%, and 15.20% of that in the world, respectively [2]. During the coal mining and washing, about 10–15% of the coal is abandoned in the form of coal gangue, in which there are 25–45% of alumina [3, 4]. The high-alumina coal gangue (HACG) with an alumina content of > 35% in ash is regarded as a potential alternative to bauxite [5].

Much work had focused on alumina extraction from HACG with a mass ratio of alumina to silica (A/S) of ~ 1.0, including alkaline methods (i.e., sintering process and hydrothermal process) and acid methods (i.e., direct leaching process and roasting-leaching process) [6–8]. A huge amount of residue (red mud), with characteristics of large specific surface area, complex composition, and strong alkalinity, are generated given the formation of Si–Ca compounds and are difficult to dispose of on land for the alkaline methods. Although the residue generation of acid methods decreases compared with that of alkaline methods, however, its disadvantages are poor solution purification, a requirement for acid-resistant and pressure equipment, and acidic wastewater treatment. In addition, the above mentioned methods cannot economically compete with the current Bayer process. However, the Bayer process is unsuitable to extract alumina from minerals with  $A/S < 6.25$  because of the formation of sodium aluminosilicate hydrates during digestion [9].

The alumina in leaching residue with  $A/S > 10$  can be extracted by the Bayer process if more than 90% of silica in HACG will be removed. Therefore, a novel technology of hematite ( $\text{Fe}_2\text{O}_3$ ) involved roasting-alkaline leaching-Bayer digestion process is proposed to extract the silica and alumina in HACG [10, 11]. Kaolinite, the main mineral in HACG, is converted to hercynite ( $\text{FeAl}_2\text{O}_4$ ) and silica solid solutions (i.e., quartz solid solution and cristobalite solid solution) through reduction roasting with hematite, then the hercynite is oxidized into hematite and alumina during the cooling process. Through leaching with sodium hydroxide solution at ~ 110 °C, more than 90% of

silica is leached to solution. The alumina in residue with  $A/S > 10$  was extracted by Bayer digestion at ~ 260 °C, and the hematite in red mud was recycled by physical separation. However, the disposal of alkali-silicate solution faces the following problems: (1) the circulation of sodium hydroxide solution is huge because the solution has low silica content; (2) large amounts of calcium hydroxide is generated, however, difficult to use when treating the alkali-silicate solution by adding lime. Thus, new attempts are suggested for the high-value application of silica in HACG.

Sodium silicate solution is an aqueous solution of sodium silicate ( $\text{Na}_2\text{O} \cdot n\text{SiO}_2$ ,  $n$  denotes modulus) and is widely used as a binder in building materials preparation, dispersing agent in flotation, decoloring agent in the sugar industry and functional silicon material [12–14]. Currently, by roasting the mixture of sodium carbonate and quartz at 1200–1400 °C and then dissolving it in water, a sodium silicate solution with a modulus of > 2.5 is obtained, whereas a sodium silicate solution with a modulus of  $\leq 2.5$  can be directly prepared by dissolving quartz into sodium hydroxide solution at ~ 170 °C [12]. In this work, to obtain the sodium silicate solution with a modulus of ~ 2.5 and alumina concentrate with  $A/S > 10$ , the alkaline leaching behavior of silica solid solutions is systematically studied in sodium hydroxide solution and sodium silicate solution. The phase transformation was investigated by X-ray diffraction (XRD), X-ray photoelectron spectroscopy (XPS), scanning electronic microscope (SEM), and energy dispersive spectrometer (EDS).

## Experimental

### Materials

In this work, the HACG used is obtained from Jungar Banner, Inner Mongolia, China, and the hematite with analytically pure ( $\text{Fe}_2\text{O}_3 \geq 99.0\%$ ) is purchased from Sinopharm Chemical Reagent Co., Ltd. The proximate analysis of the HACG indicated that there were 77.59% of ash, 15.87% of volatile matters, 5.32% of fixed carbon and 1.22% of moisture. The chemical compositions of the HACG ash were 52.44% of  $\text{SiO}_2$ , 45.21% of  $\text{Al}_2\text{O}_3$ , 0.48% of  $\text{Fe}_2\text{O}_3$ , 0.43% of CaO, 0.41% of  $\text{TiO}_2$ , and 0.25% of  $\text{Na}_2\text{O}$ . The XRD pattern indicated that kaolinite was the main mineral in the HACG and hematite had good crystallinity, as shown in Fig. 1.

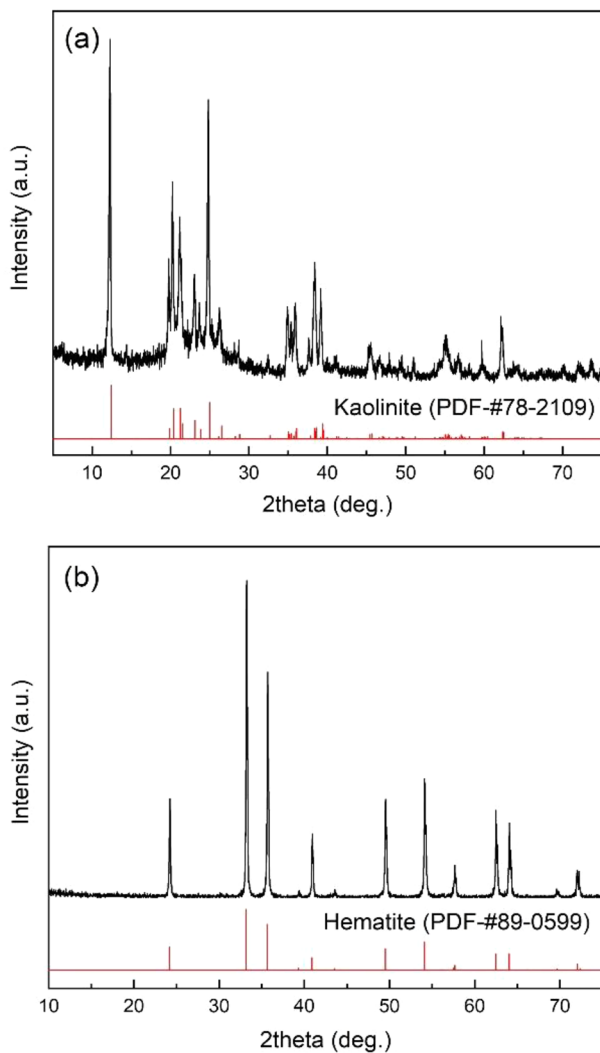


Fig. 1 XRD patterns of HACG (a) and hematite (b)

## Procedures

The hematite and HACG with  $\text{Fe}_2\text{O}_3/\text{Al}_2\text{O}_3$  molar ratio of 1.2:2.0 were well mixed in RK/XZM-100 vibrating mill for 2 min [15]. The roasting experiments were conducted in SK-G06123K controlled atmosphere resistance furnace. The furnace was heated to 1100 °C, and then injected with  $\text{N}_2$  to exhale  $\text{O}_2$ . Afterward, a 50 mL boat-type corundum crucible with 20 g of hematite and HACG mixture was put in the furnace and roasted for 60 min. The obtained reductively roasted product was called clinker. When the reduction roasting time was reached, the clinker was oxidize by injecting the air with a velocity of 500 mL/min into the furnace for 20 min, and the obtained product was oxidized clinker-1100 °C. It should be noted that, after roasting at 1100 °C for 60 min, the furnace temperature was initially reduced to 1000 °C, then the air was injected

into the furnace to oxidize the clinker for 20 min, and the obtained product was oxidized clinker-1000 °C.

The alkaline leaching of silica solid solutions were performed in a GS-0.10 high-pressure reactor (Weihai Dingda Chemical Machinery Co., Ltd, China). A certain amount of oxidized clinker was added into the high-pressure reactor together with 100 mL of sodium hydroxide solution or sodium silicate solution, then the high-pressure reactor was sealed and heated to a preset temperature. The high-pressure reactor was immediately cooled down using tap water when the reaction time was reached. Eventually, the lixivium and leaching residue were obtained by solid–liquid separation. The two-stage alkaline leaching was also conducted in the high-pressure reactor. A 10 g of leaching residue from oxidized clinker and 50 mL of sodium hydroxide solution or sodium silicate solution were added into the high-pressure reactor and reacted at 110 °C for 120 min. In addition, the sample of leaching residue (alumina concentrate) was also obtained by solid–liquid separation.

## Analyses

MAX-RB diffractometer (Rigaku Co., Japan) recorded the XRD patterns of clinker, oxidized clinkers, and leaching residues with  $\text{Cu-K}\alpha$  radiation in the  $2\theta$  range 5–80°. The XPS analysis of oxidized clinkers was performed using ESCALAB 250XI XPS (Thermo Fisher Scientific, USA). Using JXA-8230 SEM (Rigaku Co., Japan) and X-Act EDS (INCA, UK) performed the surface microscopic morphology and elemental analysis of the clinker, oxidized clinkers, leaching residues, and alumina concentrates. The  $\text{Na}_2\text{O}_k$ , which denotes the caustic soda, in solution was measured by volumetric analysis [16]. Meanwhile, a flame photometer (AP1302, AOPU, China) measured the  $\text{Na}_2\text{O}$  content in the leaching residue. Volumetric analysis and molybdenum blue colorimetry with a visible spectrophotometer (L2, INESA, China) measured the  $\text{Al}_2\text{O}_3$  and  $\text{SiO}_2$  contents, respectively. The silica leaching ratio was calculated using Eq. (1).

$$\eta = \frac{c_1 m_1 - c_2 m_2}{c_1 m_1} \times 100, \quad (1)$$

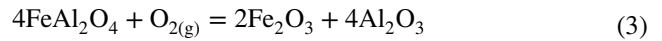
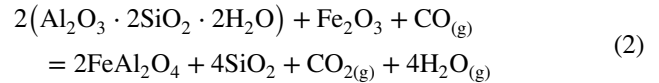
where  $\eta$  is the silica leaching ratio, %;  $c$  is the silica content, wt%;  $m$  is the mass, g; 1 and 2 represent the raw material and leaching residue, respectively.

## Results and Discussion

### Reaction Behavior of HACG and Hematite During Roasting

The XRD patterns of clinker and oxidized clinkers are shown in Fig. 2. As shown in Fig. 2a, hercynite, cristobalite solid solution, and quartz solid solution are the main minerals in the clinker, which indicates that kaolinite can efficiently react with hematite during the reduction roasting according to Eq. (2) [15]. Compared with Fig. 2a, the XRD peaks of cristobalite solid solution and quartz solid solution had no significant change after the oxidation, however, the XRD peaks of hercynite vanished and those of hematite

and alumina (i.e.,  $\theta$ -Al<sub>2</sub>O<sub>3</sub> and  $\alpha$ -Al<sub>2</sub>O<sub>3</sub>) appeared in Fig. 2b. Therefore, hercynite was oxidized into hematite and alumina according to Eq. (3) [17]. In addition,  $\theta$ -Al<sub>2</sub>O<sub>3</sub> could be further converted into  $\alpha$ -Al<sub>2</sub>O<sub>3</sub> with oxidation temperature increasing from 1000 to 1100 °C. Notably, no Al-Si compounds were found in the oxidized clinkers.



The Si2p XPS spectra of the clinker and oxidized clinker-1100 °C are shown in Fig. 3. Notably, the characteristic spectra of cristobalite and quartz were found in Fig. 3,

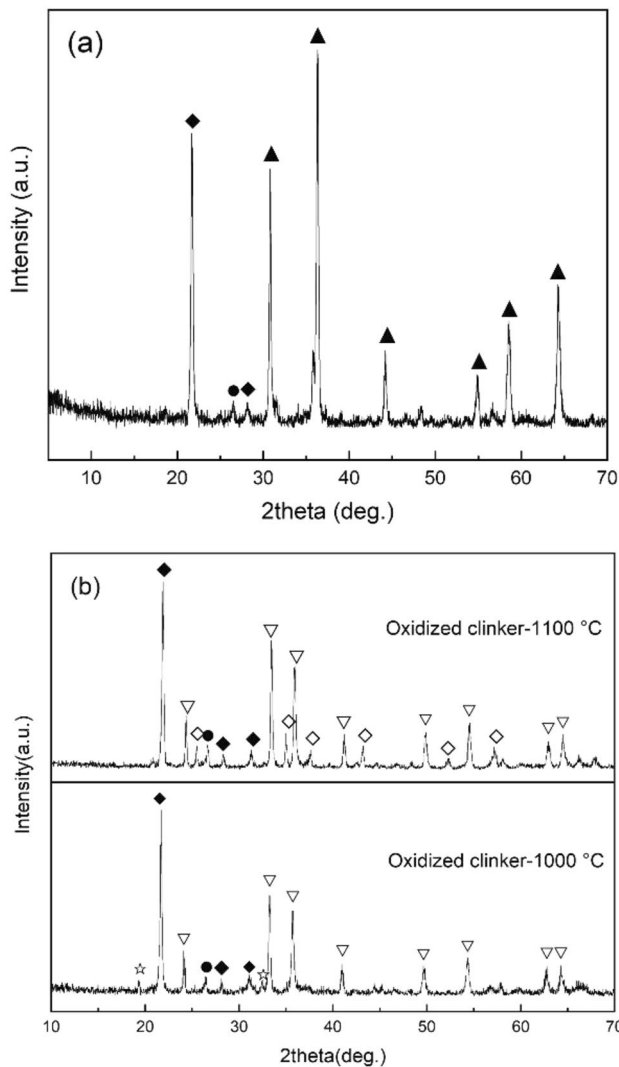


**Fig. 2** XRD patterns of clinker (a) and oxidized clinkers (b). Symbols: ▲—Hercynite, ●—Quartz solid solution; ◆—Cristobalite solid solution; ▽—Hematite; ☆— $\theta$ -Al<sub>2</sub>O<sub>3</sub>; ◇— $\alpha$ -Al<sub>2</sub>O<sub>3</sub>

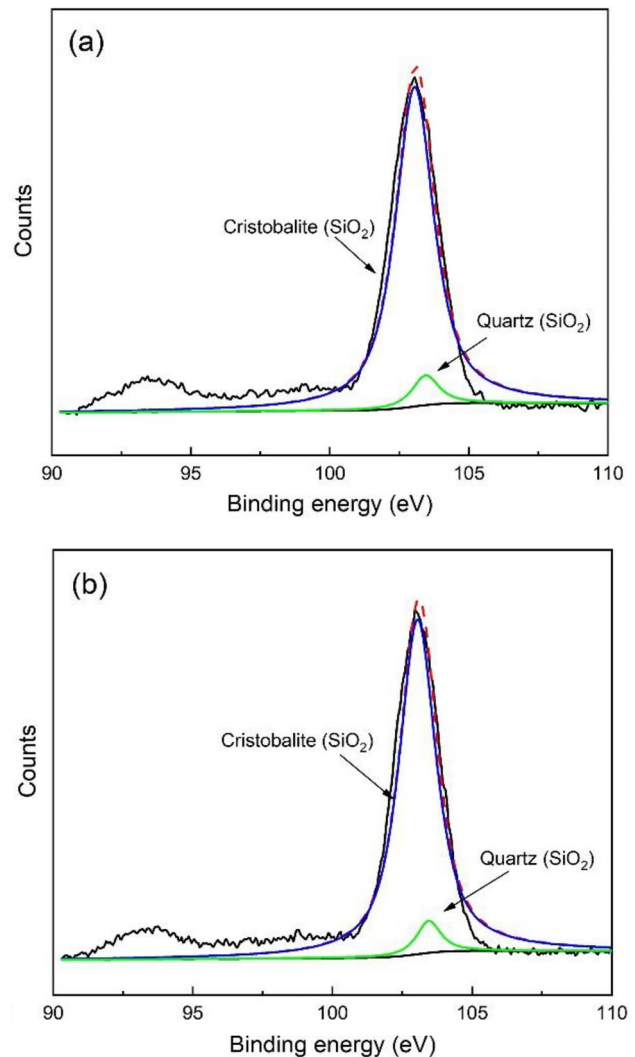


**Fig. 3** Si2p XPS spectra of clinker (a) and oxidized clinker-1100 °C (b)



however the Si-bearing minerals in clinker and oxidized clinkers were cristobalite solid solution and quartz solid solution as shown in Fig. 2. Therefore, cristobalite solid solution has the same characteristic spectrum as cristobalite, and quartz solid solution had the same characteristic spectrum as quartz. Figure 3a indicated that cristobalite solid solution and quartz solid solution were the main Si-bearing minerals in the clinker, which was consistent with those in Fig. 2a. In the oxidized clinker-1100 °C (Fig. 2b), cristobalite solid solution and quartz solid solution were still the main Si-bearing minerals and no change was observed with a comparison of those in Fig. 2a, which means that, Al–Si compounds could not be formed during the oxidation process of the clinker even at 1100 °C for 30 min.

The SEM–EDS images of the clinker and oxidized clinker-1100 °C are shown in Fig. 4. As shown in Fig. 4a, the kaolinite could be fully converted into hercynite and silica solid solutions during reduction roasting with hematite

because the Fe, Al, and Si elements are uniformly dispersed in the clinker. An iron oxide layer could be found in the particle surface of oxidized clinker-1100 °C, whereas, the Fe, Al, and Si elements in the particle interior were still uniformly dispersed. Therefore, the iron in hercynite migrated to the particle surface during oxidation roasting, thus, avoiding further reaction between alumina and silica solid solutions [17].

### Leaching Behavior of Silica Solid Solutions in Sodium Hydroxide Solution

The reaction behavior of silica solid solutions in oxidized clinker-1000 °C was investigated by leaching in the recycled solution with a NaOH concentration of 160 g/L under the conditions of 110 °C, 120 min, and solid–liquid ratio of 10 g/100 mL [18]. Results listed in Table 1 show that the content of  $\text{Na}_2\text{O}_k$ , which denotes the caustic soda in solution,

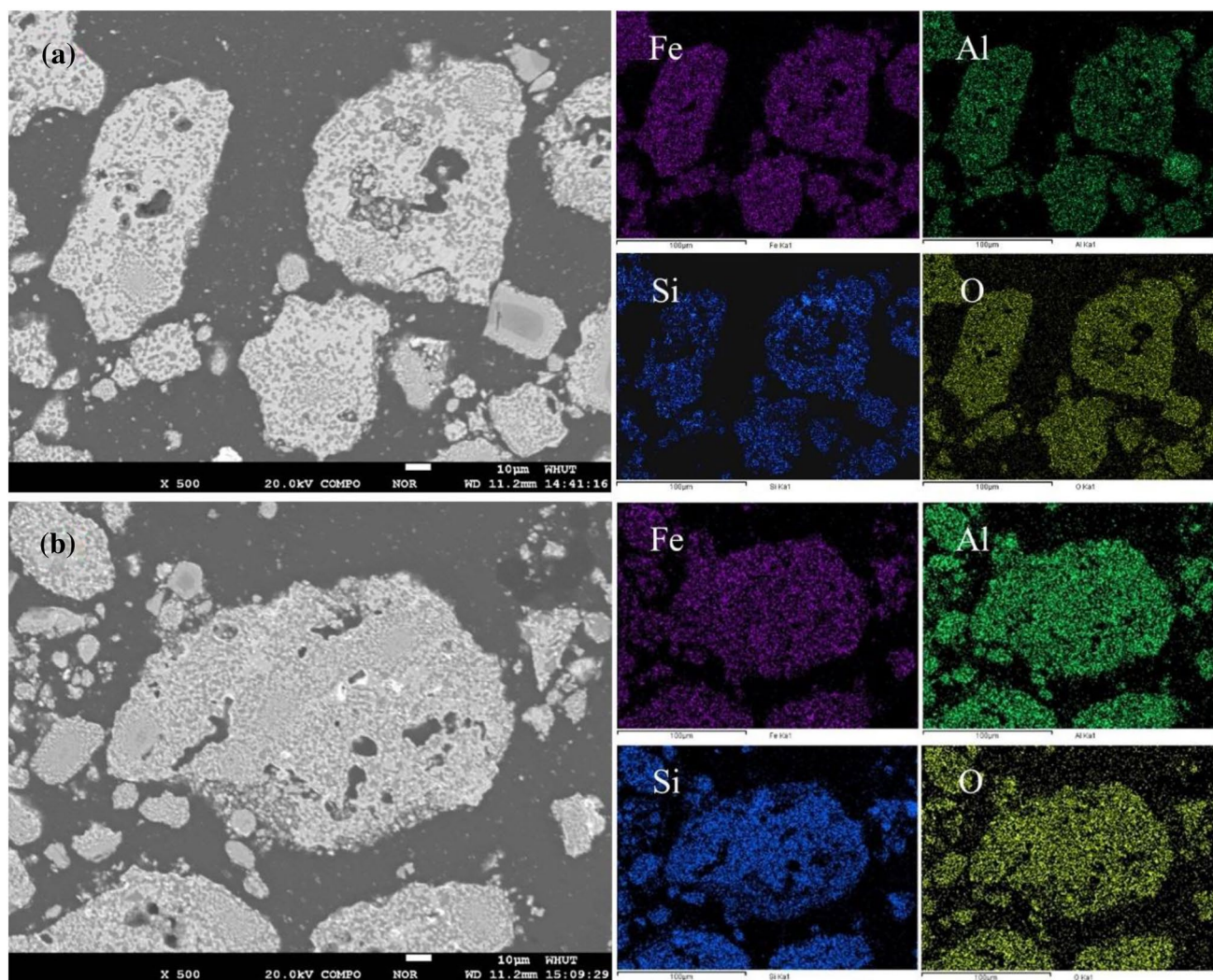
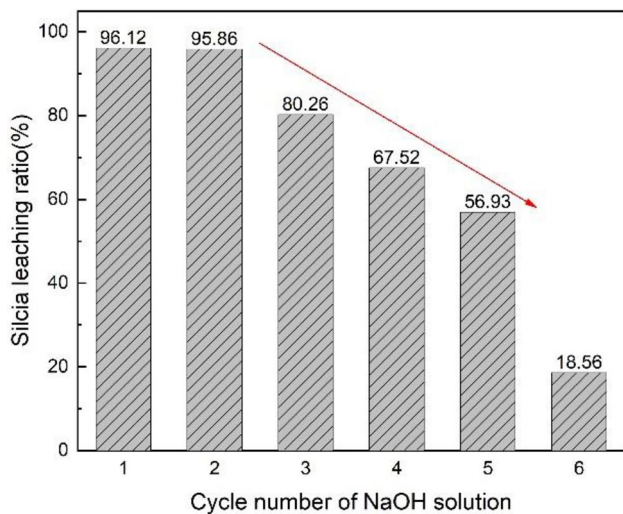


Fig. 4 SEM–EDS of clinker (a) and oxidized clinker-1100 °C (b)

**Table 1** Chemical compositions of lixivium (g/L)

	Cycle number of NaOH solution						
	0	1	2	3	4	5	6
Na <sub>2</sub> O <sub>k</sub>	123.91	117.53	110.24	108.42	105.69	101.13	99.31
SiO <sub>2</sub>	–	75.71	150.00	207.14	250.00	278.57	284.29
Al <sub>2</sub> O <sub>3</sub>	–	0.27	0.44	0.50	–	–	0.47
Modulus	–	0.67	1.41	1.97	2.44	2.85	2.96

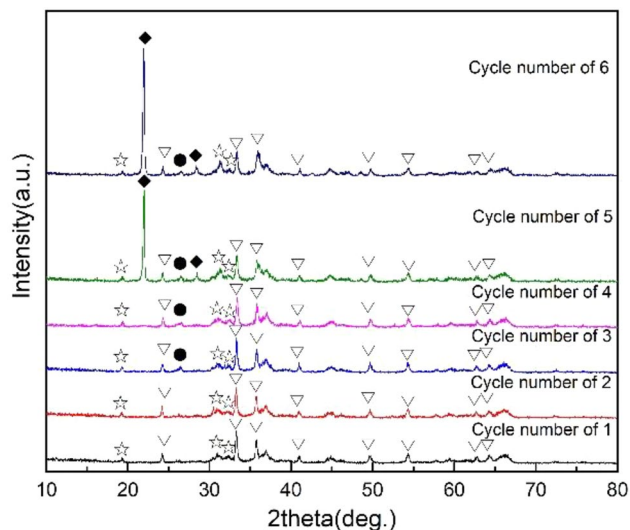
Leaching conditions: 110 °C, 120 min, solid/liquid of 10 g/50 mL, 50 mL

**Fig. 5** Silica leaching ratio at different cycle number of NaOH solution

in lixivium decreased with the sodium hydroxide solution's cycle number increase, from 123.91 g/L in sodium hydroxide solution to 99.31 g/L in lixivium with a cycle number of 6. This decreasing trend might be due to sodium ions tend to create a binding layer surrounding the silica polymeric species [19]. The SiO<sub>2</sub> content in lixivium showed an increasing trend, from 75.71 g/L in lixivium with a cycle number of 1–284.29 g/L in lixivium with a cycle number of 6. Whereas, the Al<sub>2</sub>O<sub>3</sub> content in lixivium was ≤ 0.50 g/L. Therefore, only silica solid solutions were readily soluble in sodium hydroxide solution during leaching, hence, the modulus in lixivium was increased as shown in Table 1.

The silica leaching ratio at different cycle numbers of NaOH solution are shown in Fig. 5. The silica leaching ratio was stable at ≥ 95% with the first two cycle numbers of NaOH solution, then decreased with increasing cycle numbers. Therefore, the silica solid solutions were soluble in sodium silicate solution.

As shown in Fig. 6, the XRD patterns of leaching residues indicated that the XRD peaks of cristobalite solid solution and quartz solid solution vanished after leaching with the first two cycles of NaOH solution compared with those in Fig. 2a, however, the XRD peaks of α-Fe<sub>2</sub>O<sub>3</sub> and

**Fig. 6** XRD patterns of leaching residues. ●—Quartz solid solution; ◆—Cristobalite solid solution; ▽—α-Fe<sub>2</sub>O<sub>3</sub>; ☆—θ-Al<sub>2</sub>O<sub>3</sub>

θ-Al<sub>2</sub>O<sub>3</sub> remained the same. Therefore, the silica solid solutions were dissolved into the alkaline solution, meanwhile, α-Fe<sub>2</sub>O<sub>3</sub> and θ-Al<sub>2</sub>O<sub>3</sub> were stable and enriched in the leaching residue, thus, efficient separation of silica and alumina. The cristobalite solid solution was more readily soluble in the alkaline solution than the quartz solid solution because the XRD peaks of the quartz solid solution were detected in the leaching residues with third and fourth cycle of NaOH solution. In addition, XRD peaks of cristobalite solid solution were found in the leaching residues with fifth and sixth cycle of NaOH solution, and their intensity increased with the cycle number of NaOH solution. These results indicated that dissolving the silica solid solutions into liquid solution was difficult with the increase of modulus in the lixivium, which was consistent with the leaching results in Table 1. No new Al-bearing minerals were found in the leaching residues apart from the θ-Al<sub>2</sub>O<sub>3</sub>, which means that, θ-Al<sub>2</sub>O<sub>3</sub> was stable in NaOH solution at 110 °C.

The SEM–EDS images of leaching residues with different cycle numbers of NaOH solution are shown in Fig. 7. Fe element was uniformly distributed with the Al element, whereas, the Si element become more



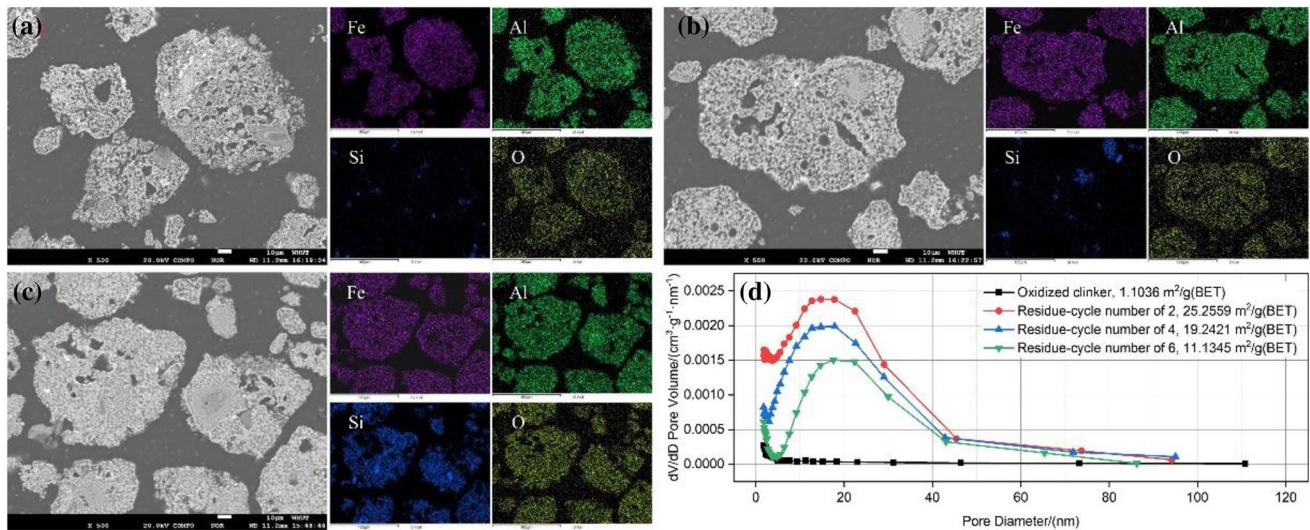


**Fig. 7** SEM–EDS images of leaching residues. **a** Cycle number of 2; **b** Cycle number of 4; **c** Cycle number of 6 and **d** Pore diameter distribution of oxidized clinker and residues

and more obvious with the increasing cycle number of NaOH solution. The silica solid solutions can be efficiently leached out into the sodium silicate solution with a modulus of  $< 1.0$ , in which the silicate mainly existed in the forms of ion or oligomer [13]. When the modulus in sodium silicate solution exceeded 2.0, polymerized silicate was the major form of silicate, thus, increasing viscosity and decreasing hydroxyl ion [20, 21]. Therefore, the higher the modulus in sodium silicate solution is, the more difficult the dissolution of silica solid solutions is. The specific surface and pore size distributions of the samples were analyzed, and the results are shown in Fig. 7d. As expected, few pores (2–50 nm) are observed in the oxidized clinker, which has a low specific surface area of  $1.1036 \text{ m}^2/\text{g}$  at models of BET surface area. The pore (2–50 nm) content increased drastically as Si was extracted during alkaline leaching, and meantime the result is a sharp increase in the specific surface area.

### Leaching Behavior of Silica Solid Solutions in Sodium Silicate Solution

The above mentioned studies indicated that the silica solid solutions were readily soluble in the NaOH solution, and the sodium silicate solution with a modulus of  $\sim 2.5$  could be obtained through the cycle of the NaOH solution. Furthermore, the sodium silicate solution with a modulus of  $\sim 2.5$  might be directly prepared by leaching the silica solid solutions in sodium silicate solution with

a modulus of 1.0 by adjusting the target modulus during leaching.

### Oxidized Clinker-1000 °C

The oxidized clinker-1000 °C and a sodium silicate solution, in which the modulus was 1.0 and  $\text{Na}_2\text{O}_k$  concentration was 100 g/L, was mixed with a target modulus of 2.0, and then leached at 110–140 °C for 1–5 h. The leaching results are presented in Fig. 8. The silica leaching ratio in Fig. 8a increased at 110 °C and 120 °C within 4 h and then decreased. The silica leaching ratio shown an increasing trend within 2 h when leaching temperature reached at 130 °C and 140 °C, and then a significant decreasing trend was observed at 2–5 h. The alumina in oxidized clinker-1000 °C might be leached out under the leaching conditions of silica solid solutions and the solid sodium aluminosilicate hydrates were formed. Thus, the silica leaching ratio shown a decreasing trend with leaching temperature and time, which could be verified through the variation trend of  $\text{Na}_2\text{O}$  content in residue as shown in Fig. 8b. The  $\text{Na}_2\text{O}$  content in leaching residues increased with leaching temperature and time. When leaching the oxidized clinker-1000 °C at 110 °C within 4 h, the  $\text{Na}_2\text{O}$  content in the residue was below 0.50%, and with a leaching time of 5 h, it increased to 0.76%. In addition, with leaching time of 1 h, the  $\text{Na}_2\text{O}$  content in leaching residues continuously increased from 0.15% at 110 °C to 0.88% at 140 °C.

The XRD patterns of leaching residues shown in Fig. 9 indicated that analcime ( $\text{Na}_2\text{O} \cdot \text{Al}_2\text{O}_3 \cdot 4\text{SiO}_2 \cdot 2\text{H}_2\text{O}$ ) was formed and its peak intensity increased with leaching

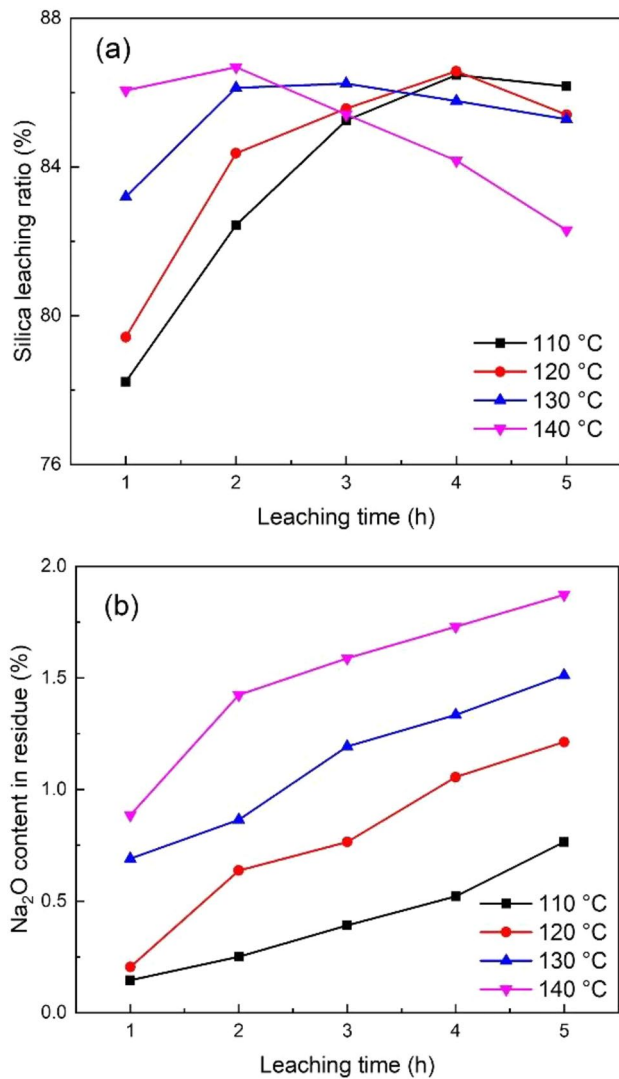


**Fig. 8** Leaching results of oxidized clinker-1000 °C in sodium silicate solution, (a) silica leaching ratio and (b) Na<sub>2</sub>O content in leaching residue. Leaching conditions: initial modulus of 1.0 and Na<sub>2</sub>O<sub>k</sub> concentration of 100 g/L, target modulus of 2.0

temperature, whereas, the peak intensity of quartz solid solution decreased with leaching temperature and ultimately vanished. Therefore, the alumina in oxidized clinker-1000 °C was not stable enough during the alkaline leaching of the silica and could react with sodium silicate solution to form analcime as shown in Eqs. (4) and (5) [22].

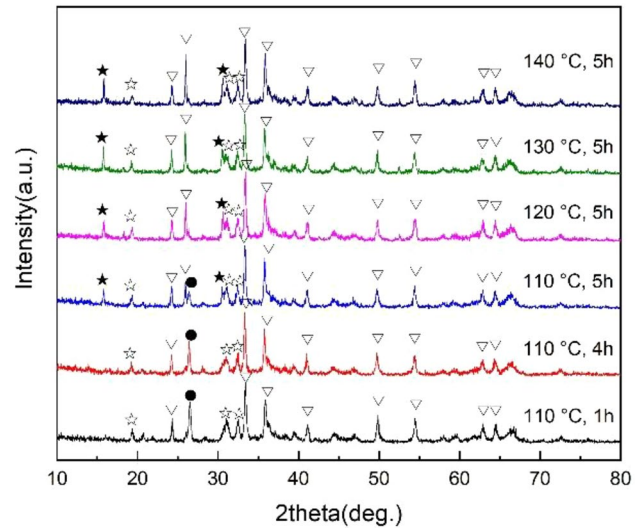
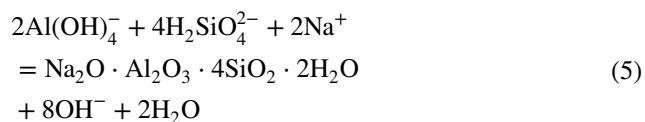


**Fig. 9** XRD patterns of leaching residues. ●—Quartz solid solution; ▽—α-Fe<sub>2</sub>O<sub>3</sub>; ☆—θ-Al<sub>2</sub>O<sub>3</sub>; ★—Analcime

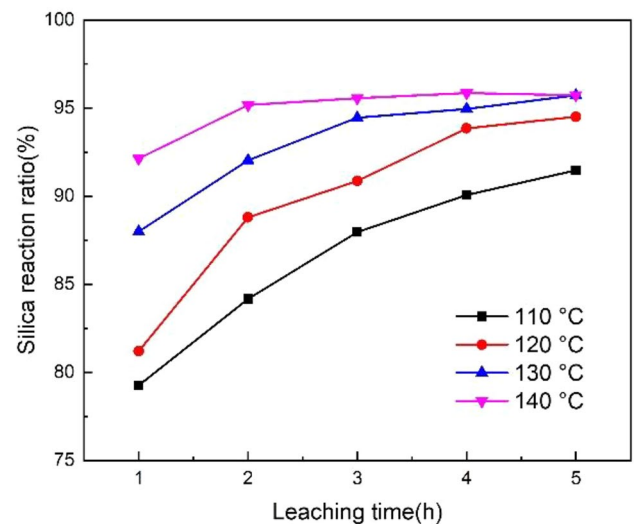


**Fig. 10** Silica reaction ratio at different leaching temperatures. Leaching conditions: initial modulus of 1.0 and Na<sub>2</sub>O<sub>k</sub> concentration of 100 g/L, target modulus of 2.0

Considering that analcime was a new product obtained during alkaline leaching, the silica in analcime could be calculated based on the Na<sub>2</sub>O content in Fig. 8b. Therefore, as shown in Fig. 10, the silica reaction ratio was calculated by adding the silica in the solution in Fig. 8a and silica in analcime. The silica reaction ratio increased with leaching time and temperature. When leached at ≤ 120 °C, the maximum silica reaction ratio was < 95% even with a leaching time of 5 h. In addition, the silica solid solutions could efficiently react with sodium silica solution with



modulus of 1.0 at  $\geq 130$  °C for  $\geq 3$  h, and the corresponding silica reaction ratio reached the maximum of  $\sim 95\%$ .

### Oxidized Clinker-1100 °C

The digestion of alumina should be avoided to increase the leaching ratio of silica in the solution. Figure 2b shows the elevated oxidation roasting temperature promoted the conversion of  $\theta\text{-Al}_2\text{O}_3$  into a more stable  $\alpha\text{-Al}_2\text{O}_3$  [23]. Thus, in this section, the leaching behavior of silica solid solutions from oxidized clinker-1100 °C was investigated in sodium silicate solution, and the results are presented in Fig. 11.

When leaching the oxidized clinker-1100 °C under the conditions: leaching temperature of 130 °C, sodium silicate solution with an initial modulus of 1.0,  $\text{Na}_2\text{O}_k$  concentration of 50 g/L and a target modulus of 3.0, the silica leaching ratio significantly increased from 61.66% for 1 h to 79.66% for 3 h, then a slowly increasing trend with time was observed as shown in Fig. 11a. When the leaching time was prolonged from 1 to 3 h, the corresponding modulus in the solution increased from 2.23 to 2.60 and the silica content in the residue decreased from 16.33 to 9.06%. In addition,  $\alpha\text{-Al}_2\text{O}_3$  was stable in the leaching conditions of silica solid solutions as indicated in the leaching results. The polymerized silicates in sodium silicate solution increased with modulus, therefore, there was a decrease of silicates in the forms of ion or oligomer [24]. Therefore, if the modulus reached a certain value, the sodium silicate solution would lose the silica's dissolving capacity. Relevant studies indicated that sodium silicate solution had a maximum modulus of  $\sim 2.5$  through alkaline leaching of quartz [12].

The silica leaching ratio and modulus in solution had a steadily increasing trend, whereas the silica content in the residue had a continually decreasing trend, if leached in sodium silicate solution with an initial modulus of 1.3 and a target modulus of 3.0 as shown in Fig. 11b. However, for 5 h, the silica leaching ratio only reached 73.24%, and the corresponding modulus in the solution and silica content in the residue were 2.25 and 11.98%, respectively. The reaction between silica and hydroxyl ion was the dissolution mechanism of silica into the sodium silicate solution [25]. The hydroxyl ion concentration in the solution decreased with the increase of modulus in sodium silicate solution, thus, the silica leaching ratio decreased with an initial modulus of 1.3.

To increase the silica leaching ratio, the target modulus was changed to 2.7 and the initial modulus was 1.0. The maximum silica leaching ratio reached 81.74% for 3 h, whereas the modulus in obtained solution was 2.40 as shown in Fig. 11c. In comparison with the results in Fig. 11a, the silica leaching ratio slightly increased, however, the modulus in the solution slightly decreased by decreasing the target modulus. Therefore, to obtain the sodium silicate solution

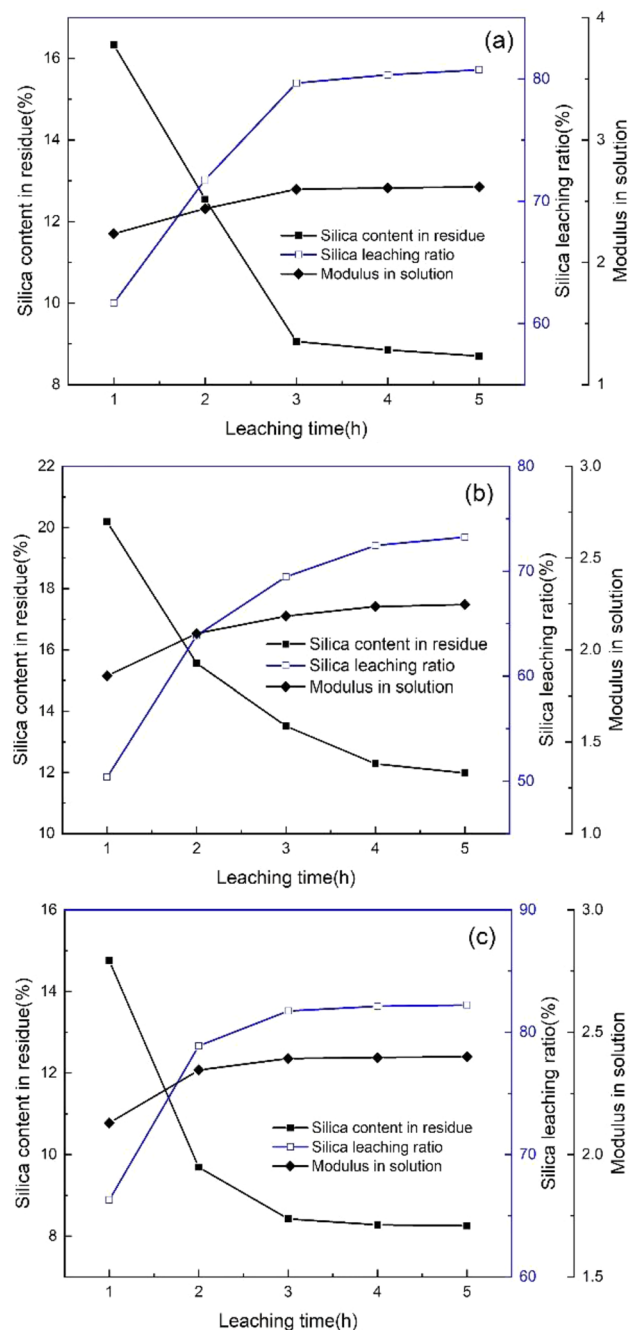


**Fig. 11** Effect of the initial modulus and target modulus of sodium silicate solution on leaching results. **a** Initial modulus of 1.0, target modulus of 3.0; **b** Initial modulus of 1.3, target modulus of 3.0; **c** Initial modulus of 1.0, target modulus of 2.7. Leaching conditions:  $\text{Na}_2\text{O}_k$  concentration of 50 g/L, temperature of 130 °C

with a modulus of  $\sim 2.5$ , the target modulus should be controlled at 3.0.

The main phases such as cristobalite solid solution,  $\alpha\text{-Fe}_2\text{O}_3$ , and  $\alpha\text{-Al}_2\text{O}_3$  were indicated by XRD patterns of the leaching residues (Fig. 12). The XRD peak intensity of the cristobalite solid solution decreased with time, hence,

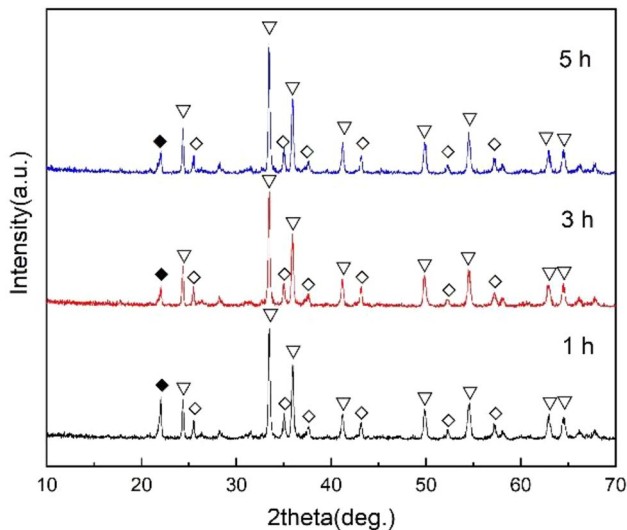


**Fig. 12** XRD patterns of leaching residues. Symbols:  $\blacklozenge$ —Cristobalite solid solution;  $\nabla$ — $\alpha$ - $\text{Fe}_2\text{O}_3$ ;  $\diamond$ — $\alpha$ - $\text{Al}_2\text{O}_3$ . Leaching conditions:  $\text{Na}_2\text{O}_k$  concentration of 50 g/L, temperature of 130 °C, initial modulus of 1.0, target modulus of 3.0

there was dissolution during leaching. In addition, given that no new Al-bearing minerals were found in the leaching residues, the  $\alpha$ - $\text{Al}_2\text{O}_3$  was stable in sodium silicate solution at 130 °C.

### Two-Stage Alkaline Leaching of Silica Solid Solutions

A sodium silicate solution with modulus of  $\sim 2.5$  was obtained through leaching the oxidized clinker-1100 °C in sodium silicate solution, in which the modulus was 1.0 and

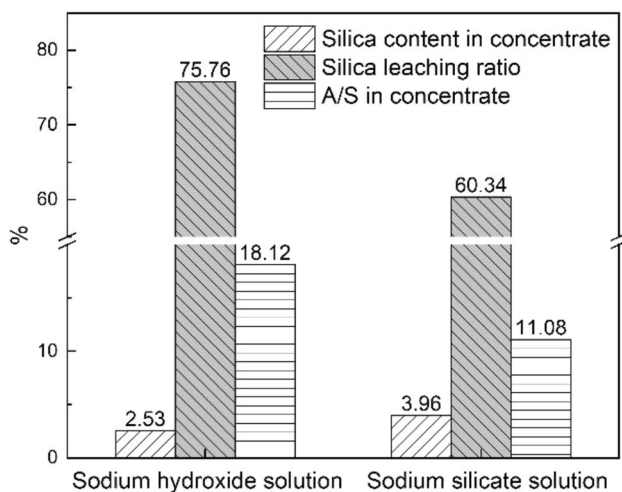
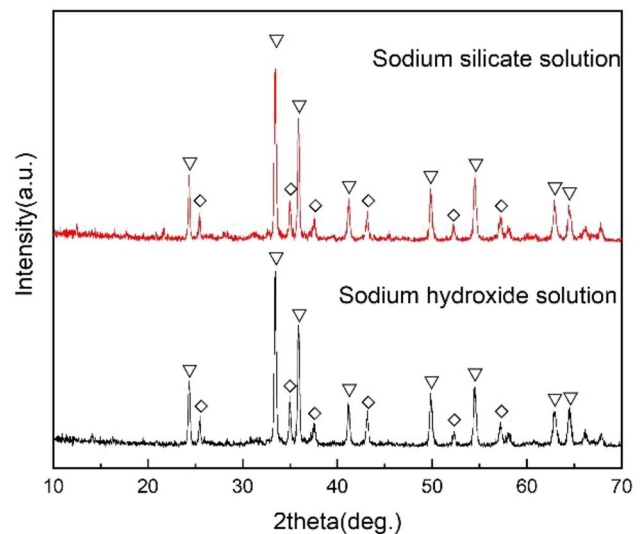


**Fig. 13** Effect of leaching agents on silica leaching results. Leaching conditions: temperature of 110 °C, 120 min, solid/liquid of 10 g/50 mL

$\text{Na}_2\text{O}_k$  concentration was 50 g/L, at 130 °C for 3 h with the target modulus of 3.0. The A/S increased from 0.86 in HACG to 4.39 in leaching residue with the removal of 79.66% silica. However, the alumina in leaching residue was difficult to be extracted by the Bayer process because of the low A/S [9]. Therefore, to further increase the A/S, a two-stage alkaline leaching was conducted by removing the silica, and the results are shown in Fig. 13.

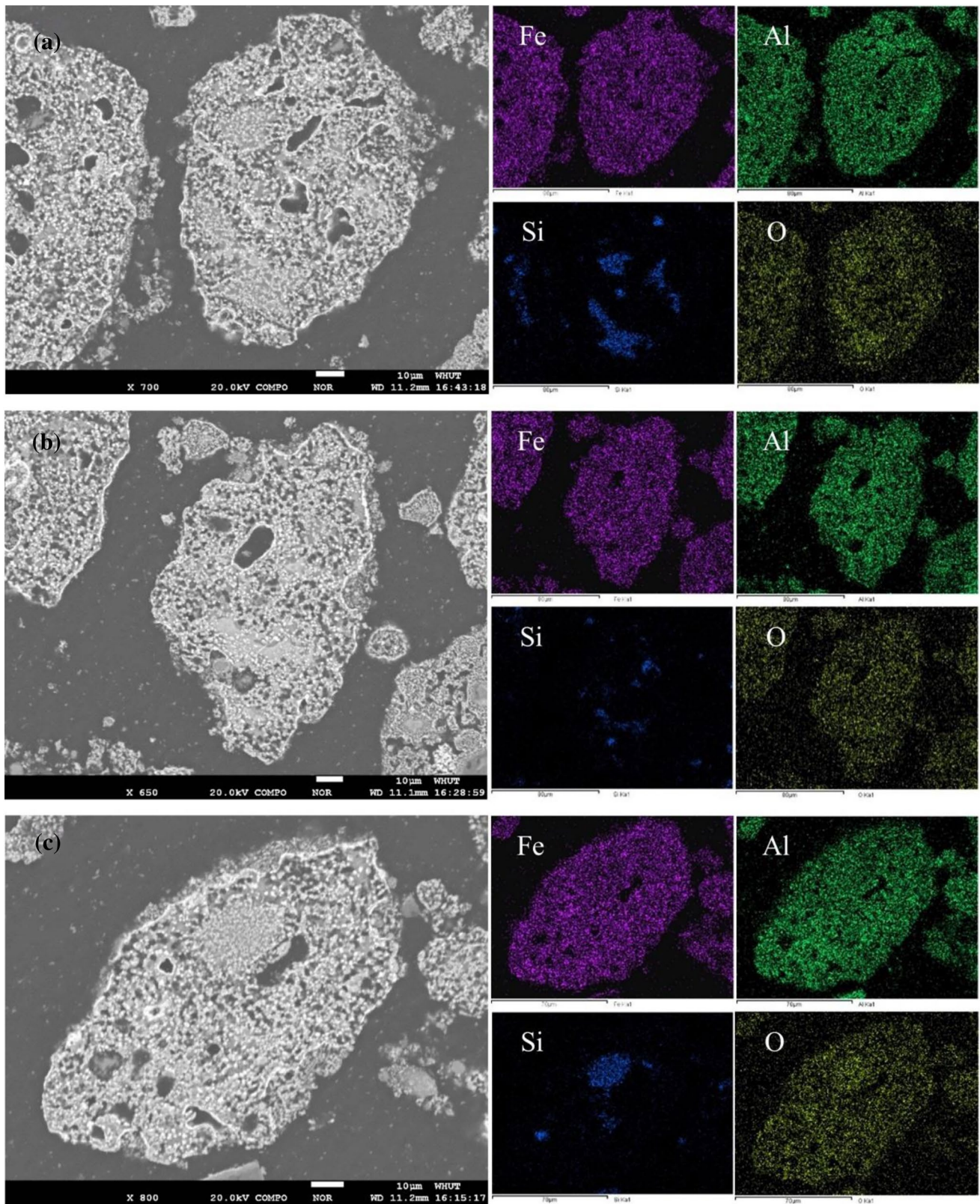
When leaching the residue in the solution with a NaOH concentration of 160 g/L, the silica leaching ratio reached 75.76% and the A/S increased to 18.12 with 2.53% silica in alumina concentrate. The A/S in alumina concentrate increased to 11.08 with the removal of 60.34% silica under the same leaching conditions, and the silica content in alumina concentrate was 3.96% by leaching in sodium silicate solution with a modulus of 1.0. Thus, sodium hydroxide solution was more suitable for removing the silica in the residue because of the higher silica leaching ratio. In addition, the cristobalite solid solution was further leached out with a two-stage alkaline leaching as indicated by XRD patterns of alumina concentrate (Fig. 14). Moreover,  $\alpha$ - $\text{Fe}_2\text{O}_3$  and  $\alpha$ - $\text{Al}_2\text{O}_3$  were the main minerals in alumina concentrate.

Figure 15 shows the SEM–EDS images of leaching residue and alumina concentrate. From Fig. 15a, the particles had porous structures because of the alkaline leaching of silica, and the remaining silica mainly existed in the particle interior. After leaching in sodium hydroxide solution, the silica in the residue was completely removed as shown in Fig. 15b, meanwhile, a small amount of silica could be found in the alumina concentrate from sodium silicate solution as shown in Fig. 15c. Given that, the migration of



**Fig. 14** XRD patterns of alumina concentrates. Symbols:  $\nabla$ — $\alpha$ - $\text{Fe}_2\text{O}_3$ ;  $\diamond$ — $\alpha$ - $\text{Al}_2\text{O}_3$ . Leaching conditions: temperature of 110 °C, 120 min, solid/liquid of 10 g/50 mL

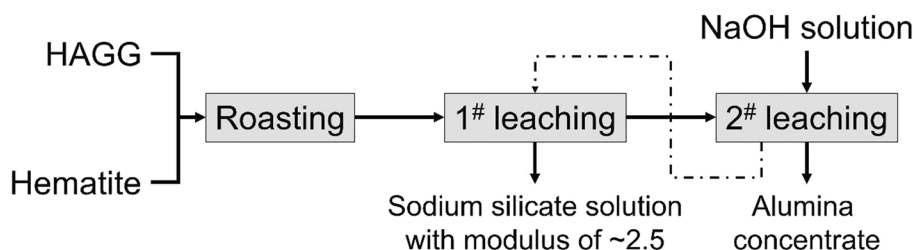




**Fig. 15** SEM–EDS images of leaching residue (a), alumina concentrate from sodium hydroxide solution (b), and alumina concentrate from sodium silicate solution (c)



**Fig. 16** Principle flow sheet of alkaline leaching of silica solid solutions



sodium silicate solution with a modulus of  $> 1.0$  into sodium hydroxide solution was faster than that into sodium silicate solution with a modulus of  $1.0$ , which was formed in the silica interface during leaching,

Therefore, the full conversion of kaolinite into silica solid solutions (i.e., quartz solid solution and cristobalite solid solution) and alumina (i.e.,  $\theta\text{-Al}_2\text{O}_3$  and  $\alpha\text{-Al}_2\text{O}_3$ ) could be obtained by roasting with hematite, and a more stable  $\alpha\text{-Al}_2\text{O}_3$  was formed in the oxidized clinker- $1100\text{ }^\circ\text{C}$ . During alkaline leaching, the sodium silicate solution with a modulus of  $\sim 2.5$  was obtained by leaching the oxidized clinker- $1100\text{ }^\circ\text{C}$  in sodium silicate solution with a modulus of  $1.0$ , then the alumina concentrate with  $A/S > 18.0$  was prepared through leaching the residue in sodium hydroxide solution. Thus, the principle flow sheet of alkaline leaching of silica solid solutions from roasting the mixture of HACG and hematite was proposed and drawn in Fig. 16. The alumina concentrate with  $A/S > 18.0$  was a decent raw material for alumina extraction by the Bayer process, and the sodium silicate solution with a modulus of  $\sim 2.5$  could be used in the chemical industry.

## Conclusions

In this work, the alkaline leaching behavior of silica solid solutions in the product obtained by roasting the mixture of HACG and hematite was systematically studied in sodium hydroxide solution and sodium silicate solution, and the main conclusions are listed below.

- (1) Through the reduction roasting with hematite at  $1100\text{ }^\circ\text{C}$  for 60 min, kaolinite, which was the main mineral in HACG, could be fully converted into hercynite and silica solid solutions (i.e., quartz solid solution and cristobalite solid solution). In addition, the hercynite was oxidized into hematite and alumina (i.e.,  $\theta\text{-Al}_2\text{O}_3$  and  $\alpha\text{-Al}_2\text{O}_3$ ) during the cooling process, elevating the oxidation temperature, hence, promoting the conversion of  $\theta\text{-Al}_2\text{O}_3$  into more stable  $\alpha\text{-Al}_2\text{O}_3$ .
- (2) The quartz solid solution and cristobalite solid solution could be completely dissolved into sodium hydroxide solution, meanwhile alumina and hematite remained stable. Therefore, the silica in oxidized clinker was

selectively removed by alkaline leaching, and the sodium silicate solution with modulus of  $\sim 2.5$  was obtained through the cycle of sodium hydroxide solution.

- (3) The sodium silicate solution with a modulus of  $\sim 2.5$  and alumina concentrate with  $A/S > 18.0$  were obtained by leaching the oxidized clinker- $1100\text{ }^\circ\text{C}$  in sodium silicate solution with a modulus of  $1.0$  as a one-stage leaching agent followed in sodium hydroxide solution as two-stage leaching agent. The alumina concentrate was a decent raw material for alumina extraction by the Bayer process.

**Acknowledgements** This work was financially supported by the National Natural Science Foundation of China (Grant No. 52004194) and the Postdoctoral Research Foundation of China (Grant No. 2019M662733).

## Declarations

**Conflict of interest** The authors declare that they have no conflict of interest.

## References

1. United States Geological Survey (USGS) (2020) Mineral commodity summaries: bauxite and alumina. <https://pubs.usgs.gov/periodicals/mcs2020/mcs2020-bauxite-alumina.pdf>
2. Thomas LP (2013) Coal resources and reserves. In: Osborne D (ed) The coal handbook: towards cleaner production. Woodhead Publishing, Sawston, pp 80–106
3. Li J, Wang J (2019) Comprehensive utilization and environmental risks of coal gangue: a review. J Cleaner Prod 239:117946. <https://doi.org/10.1016/j.jclepro.2019.117946>
4. Moghadam MJ, Ajalloeian R, Hajiannia A (2019) Preparation and application of alkali-activated materials based on waste glass and coal gangue: a review. Constr Build Mater 221:84–98. <https://doi.org/10.1016/j.conbuildmat.2019.06.071>
5. Li F, Fang Y (2016) Ash fusion characteristics of a high aluminum coal and its modification. Energy Fuels 30(4):2925–2931. <https://doi.org/10.1021/ACS.ENERGYFUELS.6B00285>
6. Yao ZT, Ji XS, Sarker PK et al (2015) A comprehensive review on the applications of coal fly ash. Earth Sci Rev 141:105–121. <https://doi.org/10.1016/j.earscirev.2014.11.016>
7. Valeev D, Bobylev P, Osokin N et al (2022) A review of the alumina production from coal fly ash, with a focus in Russia. J

- Clean Prod 363:132360. <https://doi.org/10.1016/j.jclepro.2022.132360>
8. Xiao J, Li F, Zhong Q et al (2015) Separation of aluminum and silica from coal gangue by elevated temperature acid leaching for the preparation of alumina and SiC. *Hydrometallurgy* 155:118–124. <https://doi.org/10.1016/j.hydromet.2015.04.018>
  9. Smith P (2009) The processing of high silica bauxites—review of existing and potential processes. *Hydrometallurgy* 98(1–2):162–176. <https://doi.org/10.1016/j.hydromet.2009.04.015>
  10. Li XB, Wang HY et al (2019) Efficient separation of silica and alumina in simulated CFB slag by reduction roasting-alkaline leaching process. *Waste Manag* 87:798–804. <https://doi.org/10.1016/j.wasman.2019.03.020>
  11. Wang H, Zhang X, Liu C et al (2021) Comprehensive extraction of silica and alumina from high-alumina coal gangue (HACG): hematite involved roasting—alkaline leaching—Bayer digestion process. *J Sustain Metall* 7(4):1686–1698. <https://doi.org/10.1007/s40831-021-00433-4>
  12. Vinai R, Soutsos M (2019) Production of sodium silicate powder from waste glass cullet for alkali activation of alternative binders. *Cem Concr Res* 116:45–56. <https://doi.org/10.1016/j.cemconres.2018.11.008>
  13. Lian X, Peng ZH, Shen LT et al (2021) Properties of low-modulus sodium silicate solution in alkali system. *Trans Nonferrous Met Soc China* 31(12):3918–3928. [https://doi.org/10.1016/S1003-6326\(21\)65774-6](https://doi.org/10.1016/S1003-6326(21)65774-6)
  14. Li XB, Gao XB, Wang YL et al (2022) Coal fly ash cleaner utilization by ferric oxide assisted roasting—leaching silica: recycling lixiviant by seeded precipitation of leachate. *Process Saf Environ Prot* 164:827–835. <https://doi.org/10.1016/j.psep.2022.06.068>
  15. Li XB, Wang HY, Zhou QS et al (2019) Reaction behavior of kaolinite with ferric oxide during reduction roasting. *Trans Nonferrous Met Soc China* 29(1):186–193. [https://doi.org/10.1016/S1003-6326\(18\)64927-1](https://doi.org/10.1016/S1003-6326(18)64927-1)
  16. Watts HL, Utley DW (1953) Volumetric analysis of sodium aluminate solutions. *Anal Chem* 25(6):864–867. <https://doi.org/10.1021/ac60078a005>
  17. Li XB, Wang HY, Zhou QS et al (2020) Phase transformation of hercynite during the oxidative roasting process. *JOM* 72(10):3341–3347. <https://doi.org/10.1007/s11837-020-04215-3>
  18. Wang HY, Zhang XX, Yang SY et al (2022) Separation of alumina and silica from metakaolinite by reduction roasting-alkaline leaching process: effect of CaSO<sub>4</sub> and CaO. *Trans Nonferrous Met Soc China* 32(3):999–1009. [https://doi.org/10.1016/S1003-6326\(22\)65849-7](https://doi.org/10.1016/S1003-6326(22)65849-7)
  19. Lunevich L, Sancio P, Dumeé LF (2016) Silica fouling in high salinity waters in reverse osmosis desalination (sodium-silica system). *Environ Sci Water Res* 2:539–548. <https://doi.org/10.1039/C6EW00065G>
  20. Yang XH, Zhu WL, Yang Q (2008) The viscosity properties of sodium silicate solutions. *J Solut Chem* 37(1):73–83. <https://doi.org/10.1007/s10953-007-9214-6>
  21. Nordström J, Nilsson E, Jarvol P et al (2011) Concentration- and pH-dependence of highly alkaline sodium silicate solutions. *J Colloid Interface Sci* 356(1):37–45. <https://doi.org/10.1016/j.jcis.2010.12.085>
  22. Croker D, Loan M, Hodnett BK (2008) Desilication reactions at digestion conditions: an in situ X-ray diffraction study. *Cryst Growth Des* 8(12):4499–4505. <https://doi.org/10.1021/cg8004739>
  23. Jastrzębska I, Szczerba J, Błachowski A et al (2017) Structure and microstructure evolution of hercynite spinel (Fe<sup>2+</sup>Al<sub>2</sub>O<sub>4</sub>) after annealing treatment. *Eur J Mineral* 29(1):63–72. <https://doi.org/10.1127/ejm/2017/0029-2579>
  24. Nauman RV, Debye P (1951) Light-scattering investigations of carefully filtered sodium silicate solutions. *J Phys Colloid Chem* 55(1):1–9. <https://doi.org/10.1021/j150484a001>
  25. Wang RC, Zhai YC, Ning ZQ et al (2014) Kinetics of SiO<sub>2</sub> leaching from Al<sub>2</sub>O<sub>3</sub> extracted slag of fly ash with sodium hydroxide solution. *Trans Nonferrous Met Soc China* 24(6):1928–1936. [https://doi.org/10.1016/S1003-6326\(14\)63273-8](https://doi.org/10.1016/S1003-6326(14)63273-8)

**Publisher's Note** Springer Nature remains neutral with regard to jurisdictional claims in published maps and institutional affiliations.

## Authors and Affiliations

Xiao-bin Li<sup>1</sup> · Peng Wang<sup>1</sup> · Hong-yang Wang<sup>1,2</sup> · Qiu-sheng Zhou<sup>1</sup> · Tian-gui Qi<sup>1</sup> · Gui-hua Liu<sup>1</sup> · Zhi-hong Peng<sup>1</sup> · Yi-lin Wang<sup>1</sup> · Lei-ting Shen<sup>1</sup>

✉ Hong-yang Wang  
hywang3@aust.edu.cn

✉ Yi-lin Wang  
wang.yi.lin@outlook.com

<sup>1</sup> School of Metallurgy and Environment, Central South University, Changsha 410083, Hunan, China

<sup>2</sup> School of Materials Science and Engineering, Anhui University of Science and Technology, Huainan 232001, Anhui, China